

Solar system consistency of $f(R)$ gravity theory and its MOND equivalence

Debojit Paul,^{1*} and Sanjeev Kalita,¹

¹*Department of Physics, Gauhati University, Guwahati-781014, Assam, India*

Accepted XXX. Received YYY; in original form ZZZ

ABSTRACT

Since last two decades $f(R)$ gravity theory has been extensively used as a serious alternative of general relativity to mimic the effects of dark energy. The theory presents a Yukawa correction to Newtonian gravitational potential, acting as a fifth force of Nature. Generally speaking, this new force is mediated by a scalar field known as scalaron. It affects orbital dynamics of test bodies around a central mass. When the scalaron becomes extremely massive $f(R)$ gravity reduces to Newtonian theory in the weak field limit. In this paper we test $f(R)$ gravity theory in the Solar system by constraining scalaron mass through existing measurements of perihelion shift of planets, Cassini’s measurement of the Parameterised Post Newtonian parameter and measurement of the Brans-Dicke coupling constant. We calculate acceleration due to gravity in the theory for planets, Trans Neptunian Objects (TNOs), Centaurs, Scattered Disk Objects (SDOs) and Oort cloud objects and compare it with the values predicted by Newtonian and Modified Newtonian Dynamics (MOND). It is found that the theory reproduces to MOND like acceleration in the outer Solar system ($r_p \sim 2000$ au - 36000 au) for available interpolating functions of the MOND paradigm. From its MOND equivalence we constrain the parameters of the theory. Our results are consistent with existing constraints on the theory arising from the environment of the Galactic Centre black hole.

Key words: Gravitation – Kuiper belt: general – Oort Cloud

1 INTRODUCTION

The Solar system provides us with a laboratory to test theories of gravitation. Einstein’s general relativity (GR) has been extensively tested by several independent observations and space fly-by experiments (Will 2014). It has been found to be a remarkably accurate theory of gravity in the scale of the Solar system. Testability of several general relativistic effects through very compact orbits of stars near the galactic centre black hole have been investigated by Lalremruati & Kalita (2021). Schwarzschild pericentre shift of the S2 star near the Galactic black hole and its gravitational redshift have been detected by the Very Large Telescope (GRAVITY Collaboration et al. 2018, 2020). However, in past several decades serious alternatives to GR were proposed to address the primordial singularity problem (Starobinsky 1980) and to replace mysterious dark matter and dark energy components in the standard model of cosmology (Capozziello 2002; Capozziello et al. 2007; Starobinsky 2007). Within the framework of GR dark matter and dark energy are to be included to account for origin of large scale structures (Peebles 1982; Blumenthal et al. 1984) and accelerated expansion of the universe (Sahni & Starobinsky 2000; Peebles & Ratra 2003). No laboratory experiment has been able to give satisfactory hint of expected particle candidates of dark matter (Abercrombie et al. 2020; PICO Collaboration et al. 2016; XENON Collaboration et al. 2018; The Fermi-LAT Collaboration et al. 2015; Chan & Lee 2020, 2022c,a). Dark energy is believed to be a cosmological constant – the repulsive energy density in vacuum with a negative pressure which accelerates the cosmic expansion (Riess et al. 1998; Perlmutter et al. 1999; Sahni & Starobinsky 2000;

Carroll 2001; Peebles & Ratra 2003). But the energy density of vacuum calculated in quantum theory (Weinberg 1989) is larger than the one measured from the observations of accelerated expansion of the universe (Riess et al. 1998; Perlmutter et al. 1999) by a factor of 10^{120} . This is realized to be unnatural and represents a deep puzzle in understanding of gravitation in cosmological setting. There is a plethora of dark energy models which include dynamical scalar fields carrying negative pressure and coupled dark matter –dark energy scenarios to explain the cosmic acceleration. Interested readers may like to follow excellent reviews available in literature (see e.g. Sahni & Starobinsky (2000); Peebles & Ratra (2003); Copeland et al. (2006); Amendola & Tsujikawa (2010)). Here we emphasize on the point that physics of dark energy is not yet known. Due to these reasons, it is believed that dark matter and dark energy are not exotic forms of matter-energy, rather manifestation of modification of GR in the large scale structure of the universe (Capozziello et al. 2007; Stabile & Capozziello 2013; Odintsov et al. 2023).

One of the extensively studied extensions of GR is $f(R)$ gravity theory. This is geometric modification of Einstein’s gravitational field equations. Here the Ricci scalar, R in gravitational Lagrangian is replaced by a general function of it, $f(R)$. In cosmological setting the resulting field equations modify the Friedmann-Lemaître evolution, where a curvature fluid appears leading to self accelerated expansion without adding extra negative pressure sources (Capozziello 2002; Nojiri & Odintsov 2003; Carroll et al. 2004). In the primordial universe this scenario explains occurrence of inflation without existence of extra scalar field (Starobinsky 1980). In the galactic scales $f(R)$ gravity has been found to produce flat rotation curves in Low Surface Brightness galaxies without incorporating exotic and hitherto unknown dark matter particles (Capozziello et al. 2007). These the-

* E-mail: debojitpaul645@gmail.com

ories contain an additional scalar mode of the gravitational force, known as scalaron and is defined as the derivative $\psi = df(R)/dR$. Vacuum solution of the $f(R)$ gravity field equations shows that the scalaron field alters the Schwarzschild metric – the weak and static gravitational field around spherically symmetric bodies (Kalita 2018). The gravitational potential in $f(R)$ theory contains a Yukawa correction term with $e^{-(M_\psi cr/h)}/r$ variation, where M_ψ is mass of the scalar mode, c is the velocity of light in empty space and h is Planck’s constant. This type of correction is usually known as a fifth force of Nature (Hees et al. 2017; Kalita 2018). This gets added to the usual Newtonian term with $1/r$ scaling. Testability of the theory through observation of pericentre shift of compact stellar orbits near the Galactic Centre supermassive black hole (Sgr A*) has been extensively investigated by considering astrometric capabilities of existing large telescope facilities such as the Keck, the GRAVITY interferometer in VLT and upcoming Extremely Large Telescopes (Kalita 2020, 2021; Lalremruati & Kalita 2022; Paul et al. 2023). Recently, a Kerr metric has been constructed in $f(R)$ gravity theory (Paul et al. 2024). The Kerr metric in $f(R)$ gravity has been found to possess appropriate Schwarzschild limit. For infinitely large scalaron mass black hole solutions of $f(R)$ gravity reduce to those in GR and gravitational potential reduces to Newtonian form. By considering observed bright emission ring of the Galactic Centre black hole shadow (EHT Collaboration et al. 2022) and Lense-Thirring precession of compact stellar orbits near the black hole it has been possible to deduce that for scalarons with mass in the range $(10^{-17} - 10^{-16})$ eV, $f(R)$ gravity behaves like GR (Paul et al. 2024).

Scalar fields in gravitation theory remind us of an earlier alternative to GR. It is the Brans-Dicke theory of gravity (Brans & Dicke 1961). It was formulated to satisfy Mach’s principle of inertia. It is one of a class of theories known as scalar-tensor theories. These theories contain a long range scalar field (ϕ) in addition to the spacetime metric tensor which carries the gravitational force. Departure of the theory from GR is described by the Dicke coupling constant, ω_{BD} which appears in correction terms of the gravitational Lagrangian containing the new scalar field. The weak field limit of the theory reduces to that of GR if ω_{BD} is infinitely large. The scalar field affects general relativistic prediction of Mercury’s perihelion advance, light deflection near the Sun and gravitational time delay of electromagnetic signals near massive bodies in the Solar system (Brans & Dicke 1961; Amendola & Tsujikawa 2010). The theory has been constrained through Cassini’s measurement of time delay of electromagnetic signals by putting a lower bound on the Dicke coupling constant as $\omega_{BD} > 40000$ (Will 2014). After discovery of accelerated expansion of the universe scalar-tensor theories have been invoked to generalize the cosmological constant into a time evolving dark energy component (Amendola 1999; Bartolo & Pietroni 2000).

Existence of dark matter was confirmed in 1970s by the observations of flat rotation curves of spiral galaxies (Rubin & Ford 1970; Rubin et al. 1978). The first serious alternative to dark matter appeared in a strikingly new idea proposed by Milgrom (1983). It advocated for modification of Newtonian dynamics in the outskirts of the galaxies where acceleration due to gravity falls below a critical value, $a_o \approx 10^{-10} m s^{-2}$ (Milgrom 1983; McGaugh 2020). Known as Modified Newtonian Dynamics (MOND), this theory proposes that Newton’s gravitational acceleration law $g \propto 1/r^2$ undergoes a change to $g \propto 1/r$ at large astrophysical scales. It naturally predicts constancy of rotation velocities of test bodies in spiral galaxies (Peebles 2015). The rapidity of transition from Newtonian regime to MOND regime of acceleration is governed by an interpolating function. The theory predicts that internal dynamics of a system placed in an external gravitational field (Solar system placed in the galactic

field, for example) is affected (Milgrom 2009). MOND interpolating functions have been constrained by combined Solar system and rotation curve data (Hees et al. 2015). Effect of MOND in the outer Solar system might have been confirmed. Orbital anomaly of Kuiper Belt Objects (KBOs) with semi major axes greater than 250 au was used to predict existence of an undiscovered ninth planet in the outer Solar system (Brown et al. 2004; Batygin et al. 2019). However, it has been found that MOND can successfully account for these anomalies without a ‘Planet 9’ (Brown & Mathur 2023).

Constraints on $f(R)$ gravity theory have been put by several independent investigations near the Galactic Centre black hole and in cosmological scales (Gu 2011; Xu et al. 2018; Wilson & Bean 2021; Hough et al. 2020; Bel et al. 2015; De Martino et al. 2021; Kalita 2020, 2021; Paul et al. 2023, 2024). In this paper we report constraints on the theory by estimating scalaron mass with the help of existing measurements of perihelion shift of planets, Cassini’s measurement of the Parameterised Post Newtonian (PPN) parameter and measurement of the Brans-Dicke coupling constant. Acceleration due to gravity in the theory has been calculated for planets, Trans Neptunian Objects (TNOs), Centaurs, Scattered Disk Objects (SDOs) and Oort cloud objects. Available MOND interpolating functions have been used to investigate the scale at which $f(R)$ theory shows MOND like behaviour. The plan of the paper is as follows. In section 2, we present the bounds on mass of scalarons from planetary orbits. In section 3, constraint on scalaron mass from PPN parameter and Brans-Dicke theory is presented. Section 4 presents acceleration due to gravity induced by scalarons and their MOND equivalence. We conclude with the main results and important remarks in section 5.

2 BOUND ON MASS OF SCALARONS FROM PLANETARY ORBITS

The gravitational potential in $f(R)$ gravity theory contains a Yukawa correction to Newtonian potential which has the form, (Kalita 2018)

$$V(r) = -\frac{GM}{\psi_o r} \left(1 + \frac{1}{3} e^{-M_\psi r}\right) \quad (1)$$

Here the scalaron mass M_ψ is written in the unit of $c = h = 1$. ψ_o is a dimensionless scalar field amplitude in the theory. Since $f(R) = R$ in GR, $\psi_o = df(R)/dR = 1$. The solution of vacuum field equation in $f(R)$ theory gives the following spherically symmetric and static metric (Kalita 2018).

$$ds^2 = \left[1 - \frac{2m}{r} \left(1 + \frac{1}{3} e^{-M_\psi r}\right)\right] c^2 dt^2 - \left[1 - \frac{2m}{r} \left(1 + \frac{1}{3} e^{-M_\psi r}\right)\right]^{-1} dr^2 - r^2 d\Omega, \quad (2)$$

The metric is known as Schwarzschild-scalaron (SchS) metric. For $M_\psi \rightarrow \infty$, the metric naturally reduces to general relativistic Schwarzschild limit. The metric has been extensively studied near the Galactic Centre (GC) black hole through its effect on in-plane pericentre shift of stellar orbits and the black hole shadow measurements (Kalita 2020; Kalita & Bhattacharjee 2023; Paul et al. 2023, 2024). Recently, Paul et al. (2024) constructed a Kerr metric with scalarons and found that it reduces to the SchS metric for zero angular momentum. To constrain scalarons through their effect on orbits on the Solar system we follow the differential equation of orbit of a test particle derived earlier for the SchS metric (Paul et al. 2024). The orbit equation has the following form.

Table 1. Planetary data adopted from literature (The data is adopted from Chan & Lee (2022b) and the references therein; Nyambuya (2010) for semi-major axis, eccentricity, period and Nyambuya (2010) and March et al. (2017) for perihelion shift.)

Planet	Semi-major axis a (au)	Eccentricity e	Period P (days)	Observed perihelion shift $\delta\phi$ (arcsec/century)
Mercury	0.3871	0.206	88.97	$42.9799^{+0.0030}_{-0.0006}$
Venus	0.7233	0.007	224.70	8 ± 5
Earth	1.0000	0.017	365.26	5 ± 1
Mars	1.5237	0.093	686.98	1.3624 ± 0.0005
Jupiter	5.2034	0.048	4332.59	0.070 ± 0.004
Saturn	9.5371	0.056	10759.22	0.014 ± 0.002

$$\frac{d^2u}{d\phi^2} + u = \frac{mc^2}{L^2} \left(1 + \frac{1}{3}e^{-\frac{M_\psi}{u}}\right) + 3m \left(1 + \frac{1}{3}e^{-\frac{M_\psi}{u}}\right) u^2 + \frac{mc^2 M_\psi}{3L^2} u^{-1} e^{-\frac{M_\psi}{u}} + \frac{mM_\psi}{3} u e^{-\frac{M_\psi}{u}} \quad (3)$$

Here, $m = GM_\odot/c^2$ (where M_\odot is the mass of the Sun), $u = 1/r$, and $L^2 = ma(1 - e^2)$ (a being the semi-major axis and e being the eccentricity of the orbits). In SchS geometry, the orbit of any test particle undergoes perihelion shift by an amount (Paul et al. 2024)

$$(\delta\phi)_{SchS} = (\delta\phi)_{Sch} + \frac{6\pi m}{3a(1 - e^2)} e^{-M_\psi a(1 - e^2)} + \frac{4\pi m M_\psi}{3} e^{-M_\psi a(1 - e^2)} + \frac{2\pi a^2(1 - e^2)M_\psi^2}{6} e^{-M_\psi a(1 - e^2)} + \frac{2\pi ma(1 - e^2)M_\psi^2}{6} e^{-M_\psi a(1 - e^2)} \quad (4)$$

Here, $(\delta\phi)_{Sch}$ is the Schwarzschild perihelion shift, $6\pi m/a(1 - e^2)$. The perihelion shift in the above equation is expressed in angle per period. Equation (4) can be expressed in the following transcendental form.

$$\left[AM_\psi^2 + BM_\psi + C\right] e^{-M_\psi a(1 - e^2)} + \rho = 0 \quad (5)$$

where,

$$A = \frac{2\pi a^2(1 - e^2)}{6} + \frac{2\pi ma(1 - e^2)}{6} \quad (6)$$

$$B = \frac{4\pi m}{3}$$

$$C = \frac{6\pi m}{3a(1 - e^2)}$$

$$\rho = (\delta\phi)_{Sch} - (\delta\phi)_{SchS}$$

The observational bounds on perihelion shift available for planetary orbits up to Saturn¹ are presented in Table 1. Data from Cassini (Bertotti et al. 2003) and Messenger spacecraft (Fienga et al. 2011) has provided a stringent bound on the observed perihelion shift of Mercury (March et al. 2017). This data is combined with data for rest of the five planets (Nyambuya 2010; March et al. 2017). The observed perihelion shift presented in the Table 1 are residual perihelion shift after accounting for all other planetary perturbations, quadrupole moment of the sun and Lense-Thirring effects (Park et al. 2017). Therefore, the residual perihelion shift is expected to put constraint on modified gravity effect. Under this assumption, the perihelion shift values in Table 1 are substituted for $(\delta\phi)_{SchS}$ in equation (4).

¹ For Uranus and Neptune reliable data are not available in the literature.

Table 2. Constraints on M_ψ in different planetary orbits.

Planet	Scalaron Mass M_ψ (eV)
Mercury	5.64×10^{-16}
Venus	$2.374 \times 10^{-21} - 3.273 \times 10^{-16}$
Earth	$1.67 \times 10^{-21} - 2.07 \times 10^{-16}$
Mars	1.48×10^{-16}
Jupiter	$4.02 \times 10^{-17} - 4.21 \times 10^{-17}$
Saturn	$2.26 \times 10^{-17} - 2.71 \times 10^{-17}$

Table 3. The deviation of estimated γ from Cassini bounds.

Planets	M_ψ (eV)	$ \frac{\delta\gamma}{\gamma} $
Mercury	5.64×10^{-16}	2.1×10^{-5}
Venus	$2.374 \times 10^{-21} - 3.273 \times 10^{-16}$	$0.49 - 2.09 \times 10^{-5}$
Earth	$1.67 \times 10^{-21} - 2.07 \times 10^{-16}$	$0.49 - 2.09 \times 10^{-5}$
Mars	1.48×10^{-16}	2.09×10^{-5}
Jupiter	$4.02 \times 10^{-17} - 4.21 \times 10^{-17}$	2.09×10^{-5}
Saturn	$2.26 \times 10^{-17} - 2.71 \times 10^{-17}$	2.09×10^{-5}

From Table 2 it is evident that except for Venus and Earth which have large uncertainties in perihelion shift measurement, the rest of the planets constrain scalaron mass in the range ($10^{-17} - 10^{-16}$) eV. For Venus and Earth the bound on mass of the scalarons is quite wide ($10^{-21} - 10^{-16}$) eV. The consistency of estimated mass range of scalarons is further investigated in the next section.

3 CONSTRAINT ON SCALARON MASS FROM PPN PARAMETER AND BRANS-DICKE THEORY

The PPN parameter γ measures curvature per unit mass for a massive body (in this case the Sun). It parametrises deviation from GR in weak field limit and is measured with experiments on light deflection and Shapiro time delay (Will 2014; Bertotti et al. 2003). In case of GR, the value of γ is unity. In other theories of gravity it deviates from unity (Misner et al. 1973). The PPN parameter in $f(R)$ gravity theory is given by (Amendola & Tsujikawa 2010; Kalita 2018),

$$\gamma = \frac{3 - e^{-M_\psi r}}{3 + e^{-M_\psi r}} \quad (7)$$

In the solar system, γ is constrained as $1 + (2.1 \pm 2.3) \times 10^{-5}$. This bound has been given by the measurement of Shapiro time delay performed by the Cassini spacecraft (Bertotti et al. 2003). Using scalaron masses from Table 2 and taking perihelion distance of the planets, $r_p = a(1 - e)$, the γ values are estimated for each of the planetary orbits. The deviations of these estimated values from the observed values ($|\delta\gamma/\gamma|$) have been presented in Table 3. It is seen that except for Venus and Earth the deviations of the estimated PPN parameter from the observed bound is extremely small for Mercury, Mars, Jupiter and Saturn. Scalarons with 10^{-16} & 10^{-17} eV are found to be remarkably consistent with Cassini's measurement of γ . In the following we investigate the scalaron mass by connecting the PPN parameter of $f(R)$ gravity theory with that of the Brans-Dicke theory.

As mentioned in the introduction, Brans-Dicke theory (BDT) is a certain class of scalar-tensor theories that was studied as a first serious alternative to GR. The theory is of particular interest as in the weak field limit it possesses a structure similar to that of

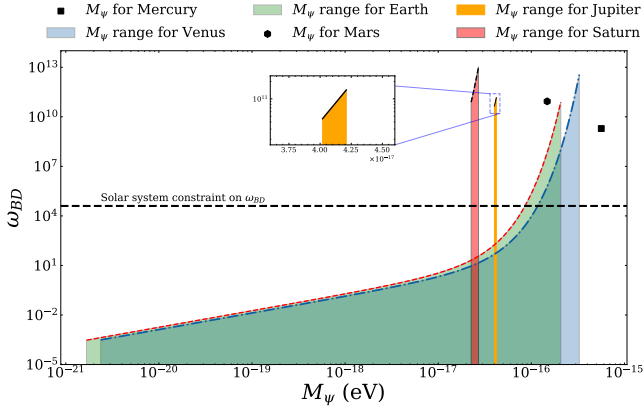


Figure 1. Variation of Dicke parameter ω_{BD} against scalaron mass M_ψ for different planetary orbits.

$f(R)$ theory. This occurs due to chameleon mechanism (Khoury & Weltman 2004)- a mechanism which allows scalaron mass to be environment dependent so that in the high density regions of planets and the Sun ($\rho \sim 10^3 - 10^4 \text{ Kg/m}^3$ which is larger than the mean cosmological density, 10^{-26} Kg/m^3) scalarons become extremely heavier and the gravitational potential (see equation (1)) looks similar to Newtonian. In BDT the gravitational constant, G is expressed in terms of reciprocal of a scalar field ϕ . The dimensionless Dicke parameter ω_{BD} measures deviation from GR. The PPN parameter in BDT is given by (Amendola & Tsujikawa 2010),

$$\gamma = \frac{1 + \omega_{BD}}{2 + \omega_{BD}} \quad (8)$$

For $\omega_{BD} \rightarrow \infty$, BDT reduces to GR ($\gamma = 1$). A very small value of ω_{BD} (~ 0) represents drastic deviation from GR with $\gamma = 1/2$. This is equivalent to zero scalaron mass in $f(R)$ theory (see equation (7)). From Cassini's measurements ω_{BD} has been constrained in the Solar system as $\omega_{BD} > 40000$ (Will 2014). Comparing equations (7) and (8) the Dicke parameter is expressed in terms of scalaron mass as

$$\omega_{BD} = \frac{3(1 - e^{-M_\psi r})}{2e^{-M_\psi r}} \quad (9)$$

For perihelion distances of the six planets the variation of ω_{BD} is studied for different scalaron masses. This variation is shown in Figure 1. It is seen that for orbits of Mercury, Mars, Jupiter and Saturn the scalaron masses derived in Table 2 are consistent with the constraint $\omega_{BD} > 40000$. Also, in the orbits of Venus and Earth much more stringent bounds on M_ψ are obtained. The bound on M_ψ for Venus is $(1.17 \times 10^{-16} - 3.27 \times 10^{-16}) \text{ eV}$. For Earth the bound is $(8.56 \times 10^{-17} - 2.07 \times 10^{-16}) \text{ eV}$.

In BDT without a scalar field potential (massless Brans-Dicke scalar field) the effective gravitational constant is given by, (Amendola & Tsujikawa 2010)

$$G_{eff} = \frac{G}{\phi_o} \left(\frac{4 + 2\omega_{BD}}{3 + 2\omega_{BD}} \right) \quad (10)$$

To relate $f(R)$ gravity with the Brans-Dicke theory we identify scalaron field as the Brans-Dicke field ($\phi_o = \psi_o$). To be compatible with measured value of Newton's constant of gravity ($G_{eff} = (6.15 \pm 0.35) \times 10^{-11} \text{ m}^3 \text{ Kg}^{-1} \text{ s}^{-2}$; (LISA Pathfinder

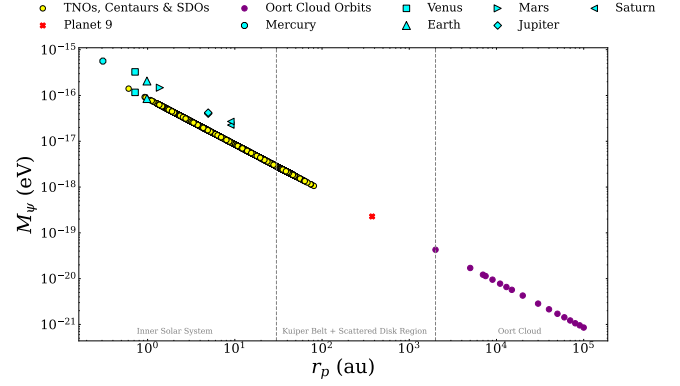


Figure 2. Variation of M_ψ with perihelion distance r_p of different orbits.

Collaboration et al. 2019)) the scalaron field amplitude ψ_o has been estimated from,

$$\psi_o = \frac{G}{G_{eff}} \left(\frac{4 + 2\omega_{BD}}{3 + 2\omega_{BD}} \right) \quad (11)$$

The scalaron field amplitude ψ_o falls in the range $\psi_o = 1.09 \pm 0.06$ for all the planetary orbits considered above. We investigate the trend of scalaron mass towards the outer solar system. The six planetary orbits, Centaurs, TNO & SDO orbits (Orbital data for TNOs, Centaurs and SDOs have been obtained from <https://www.minorplanetcenter.net/data>), orbit of hypothetical Planet 9 ($a \approx 500 \text{ au}$ & $e \approx 0.25$; Batygin et al. (2019)) and some mock Oort cloud orbits (See Appendix A) have been considered for this analysis. It is to be noted the M_ψ values for six planetary orbits have been incorporated from Table 2. But for all other orbits (TNOs, Planet 9 and Oort cloud orbits) taken into consideration, the M_ψ values have been estimated from the observational bound on γ using equation (7). The variation of M_ψ with perihelion distance (r_p) is presented in Figure 2. It is seen that the mass of the scalarons falls towards the outer solar system. In the Oort cloud scale ($r_p \sim 2000 \text{ au}$) M_ψ reaches a value $\sim 10^{-20} \text{ eV}$ and it further decreases.

4 ACCELERATION DUE TO GRAVITY INDUCED BY SCALARONS AND MOND EQUIVALENCE

As mentioned in the introduction, MOND has been studied in the outer Solar system to explain the dynamics of the KBOs. In this section we investigate the equivalence between $f(R)$ theory and MOND in the outer regimes of the Solar system. At the perihelion of the planetary orbits, the acceleration due to gravity induced by scalarons is written as,

$$g_s = - \left(\frac{dV(r)}{dr} \right)_{r_p} \quad (12)$$

Using the gravitational potential expressed in equation (1), the expression takes the form,

$$g_s = - \frac{GM}{\psi_o r_p^2} - \left(\frac{GM}{3\psi_o r_p^2} + \frac{GMM_\psi}{3\psi_o r_p} \right) e^{-M_\psi r_p} \quad (13)$$

Using equation (13) the acceleration due to gravity in the orbits of planets, TNOs/Centaurs/SDOs, Planet 9 and Oort cloud is estimated.

We take different choices of ψ_o (smaller and greater than the value 1 which is the GR case) and study the variation of acceleration due to Newtonian gravity ($g_N = -GM/r_p^2$) and acceleration due to scalaron gravity (g_s) with respect to r_p . The variations are presented in Figure 3. It is seen that the acceleration due to gravity for both Newtonian and scalaron theory fall with scale. The Newtonian acceleration g_N touches the MOND acceleration limit ($a_o = 1.2 \times 10^{-10} \text{ m/s}^2$) at around 7000 au. In case of scalaron gravity, it is seen that for lower values of ψ_o (< 1), MOND acceleration limit is reached at a larger distance as compared to the Newtonian case. On the other hand, the larger values of ψ_o (> 1) predict that the limit is reached at much smaller distances as compared to the Newtonian case. Also, it is seen that for $\psi_o \rightarrow 1$, acceleration in scalaron gravity starts converging towards the Newtonian value. We observe that for $r_p > 100$ au (the scale of the Kuiper belt objects) the acceleration due to gravity in $f(R)$ theory falls below the MOND limit. Therefore, we investigate possible equivalence of the theory with MOND.

The acceleration due to gravity in MOND is given by, (Famaey & McGaugh 2012)

$$g_M = \nu \left(\frac{g_N}{a_o} \right) g_N \quad (14)$$

Here, $\nu(x)$ represents an interpolating function (IF) that provides smooth transition from Newtonian regime to MOND regime. The IF dominates in the low acceleration limit ($g_N \ll a_o$ where $a_o \approx 1.2 \times 10^{-10} \text{ m/s}^2$ (McGaugh 2020)). For higher acceleration ($g_N \gg a_o$), $\nu(x) \rightarrow 1$. Although, no theoretical form of IF exists, the following families of IF have been extensively studied in literature (Famaey & McGaugh 2012; Hees et al. 2015).

$$\text{IF1} : \nu_\alpha(x) = \left[\frac{1 + (1 + 4x^{-\alpha})^{1/2}}{2} \right]^{1/\alpha} \quad (15)$$

$$\text{IF2} : \tilde{\nu}_\alpha(x) = (1 - e^{-x})^{-1/2} + \alpha e^{-x} \quad (16)$$

$$\text{IF3} : \bar{\nu}_\alpha(x) = (1 - e^{-x^\alpha})^{-1/2\alpha} + (1 - 1/2\alpha)e^{-x^\alpha} \quad (17)$$

$$\text{IF4} : \hat{\nu}_\alpha(x) = (1 - e^{-x^{\alpha/2}})^{-1/\alpha} \quad (18)$$

Here, α is a free parameter. The IF, $\nu_1(x)$ (commonly known as simple IF) has been extensively used in the literature as it provides smooth transition to the MOND regime (Famaey & Binney 2005; Zhao & Famaey 2006; Sanders & Noordermeer 2007; McGaugh 2008; Chae et al. 2020; Wang & Chen 2021). $\nu_2(x)$ is known as the standard IF and $\tilde{\nu}_{0.5}(x)$ has also been studied in the context of galactic dynamics (Famaey & McGaugh 2012). The $\hat{\nu}_\alpha(x)$ family, also called as δ -family IF is known to give excellent fit to rotation curve data ($\alpha = 1$) (McGaugh et al. 2016; Lelli et al. 2017; Li et al. 2018) and have been studied in the literature (Famaey & McGaugh 2012; Dutton et al. 2019; Chan & Lee 2022b). In this section, we study the variation of acceleration due to gravity with respect to scale of the outer Solar system (r_p) with all these IF families (with different choices of the parameter α) and compare it with Newtonian and scalaron counterpart. The variations are presented in Figure 4.

From Figure 4a it is seen that, the acceleration due to gravity in MOND (g_M) for IF1 family behaves as Newtonian acceleration (g_N) up to around 2000 au. Beyond this scale g_M starts deviating from g_N values and intersects the values of acceleration due to gravity

in presence of scalarons up to around 34000 au. Beyond this scale, however, g_M starts dominating the scalaron induced acceleration. In case of IF2 family (Figure 4b), it has been seen that g_M starts deviating from g_N values at around 2800 au. But for smaller values of the parameter α , g_M resembles g_s up to larger scales (~ 28000 au). For larger values of α , g_M starts dominating g_s at shorter scales (~ 7000 au). For IF3 family (Figure 4c), g_M starts deviating from g_N at around 2000 au and behaves like g_s up to 32000 au. Beyond this scale, g_M starts dominating the scalaron acceleration. Additionally it has been seen that the choice $\alpha = 0.5$ for IF3 family provides a smooth transition of acceleration due to gravity from Newtonian to scalaron gravity. Lastly, for the IF4 family (Figure 4d), the deviation from g_N starts at around 2000 au. It remains similar to g_s up to around 36000 au. Beyond this scale, g_M again starts dominating. One common feature of the four IFs is that MOND induced acceleration touches the scalaron induced acceleration for $\psi_o < 1$. Results of the significant findings are summarised below.

5 DISCUSSION AND CONCLUSION

In this work, we have tested consistency of $f(R)$ gravity with scalarons in the scale of Solar system. We have used the observational bounds on perihelion shift of inner Solar system planets (till Saturn) to constrain mass of the scalarons for these planetary orbits. The masses thus obtained have been presented in Table 2. We reproduce these masses using observational bounds on PPN parameter γ as well as the Brans-Dicke coupling constant ω_{BD} . It has been found that the scalarons in the planetary orbits have mass in the range ($10^{-17} - 10^{-16}$) eV. Also, these scalaron masses are found to uplift the minimum bound on the Dicke parameter ω_{BD} . Hence, $f(R)$ theory is found to be consistent with GR in the inner Solar system. Constraint on the parameter ψ_o has been obtained in the inner Solar system. It lies in the range $\psi_o = 1.09 \pm 0.06$ which again resembles general relativistic prediction, $\psi_o = 1$.

The theory is further tested in the regimes of the outer Solar system. Orbits of Trans Neptunian Objects, Centaurs, SDOs, hypothetical Planet 9 as well as some mock Oort cloud objects (see Appendix A) have been considered. The mass of the scalarons in each of these orbits has been estimated using the observational bound on PPN parameter γ . It has been seen that the mass of the scalarons decreases with increasing scale of the Solar system (see Figure 2). In the inner Oort cloud (~ 2000 au) the mass of the scalarons touches 10^{-20} eV. It reduces to 10^{-22} eV towards the edge of the Oort cloud (~ 100000 au).

Finally we test equivalence of $f(R)$ theory with the MOND paradigm. The acceleration due to gravity in $f(R)$ gravity theory (g_s) and Newtonian gravity (g_N) have been compared for different choices of ψ_o against perihelion distance, r_p (see Figure 3). It has been found that g_N touches MOND like acceleration ($a_o \approx 1.2 \times 10^{-10} \text{ m/s}^2$) at around 7000 au. However, in case of $f(R)$ scalarons with small values of ψ_o ($\psi_o \sim 0.2$) g_s touches MOND acceleration limit far deeper in the Oort cloud. On the other hand, higher values of ψ_o (> 1) predict that g_s touches the MOND limit at much shorter distances (outer Kuiper belt scales). For $\psi_o \rightarrow 1$, scalaron gravity induced acceleration touches the Newtonian values. It is evident that any MOND behaviour of $f(R)$ gravity is likely to manifest in Oort cloud like scales. Hence, g_N and g_s are further compared with acceleration due to gravity in MOND (g_M) for different family of IFs (see Figure 4). It is seen that for all four families of IFs considered in the study, g_M behaves as g_N till Oort cloud like scales (~ 2000 au) beyond which it starts deviating. As we probe deeper into the Oort cloud

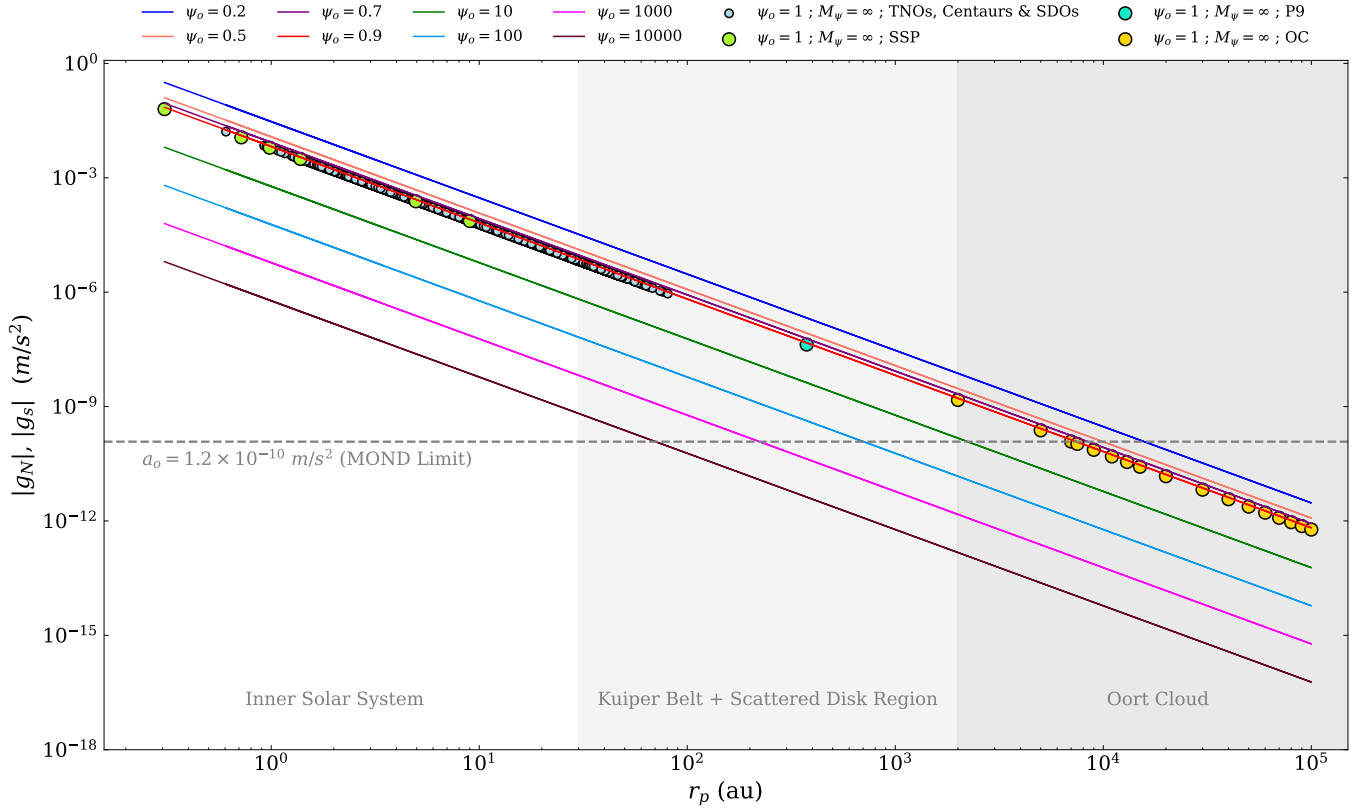


Figure 3. Variation of acceleration due to gravity in Newtonian and scalaron gravity with perihelion distance (r_p) for different planetary orbits, SDOs, Centaurs, TNOs and Mock Oort cloud orbits (The scatter points represent g_N ($\psi_o = 1$; $M_\psi = \infty$) values for each of the orbits; SSP → Orbits of Solar system planets till Saturn; P9 → orbit of Planet 9; OC → orbits of Oort cloud).

regions the MOND acceleration touches the $f(R)$ gravity regime for lower values of the scalaron field amplitude ψ_o . The IF2 family shows interesting behaviour. For higher value of the parameter α the MOND acceleration mimics the scalaron induced acceleration at much shorter scale, almost the one of the Kuiper belt objects (see Figure 4b). For this family we also observe that MOND mimics $f(R)$ gravity acceleration up to around 32000 – 36000 au. For all the IFs it is a common feature that $f(R)$ gravity and MOND show equivalence for smaller values of ψ_o . MOND dominates scalaron induced acceleration for much larger scales, the ones towards the outer Oort cloud.

10^{-16} eV scalarons were earlier predicted to exist near the horizon of the Galactic Centre black hole which affect pericentre shift of compact stellar orbits near the black hole (Kalita 2020). In a recent study Paul et al. (2024) reported that these scalarons show GR like behaviour of the gravity theory by reproducing angular size of the bright emission ring of the Galactic black hole shadow. Further, Paul et al. (2023) showed that relatively lighter scalarons with $10^{-22} - 10^{-19}$ eV can affect Schwarzschild pericentre shift of orbits of stars like S2 which will be detectable by astrometric capabilities of existing large telescopes and upcoming Extremely Large Telescopes. Therefore, scalaron masses constrained in the Solar system are compatible with those studied near the Galactic centre black hole.

We conclude with the following lines. $f(R)$ gravity theory with scalarons is found to be consistent in the Solar system. In the inner Solar system the theory reduces to GR with scalaron mass $10^{-17} - 10^{-16}$ eV. Near the inner Oort cloud regions scalaron mass is found to decrease upto 10^{-20} eV. It decreases further up to 10^{-22} eV

towards the edge of the Oort cloud. $f(R)$ theory and MOND are dynamically equivalent in the outer Solar system. It has been possible to extract a mass range of the $f(R)$ gravity degree of freedom which is compatible with the mass range of $f(R)$ derived from the effect of the theory at the neighbourhood of the Galactic Centre black hole. The MOND- $f(R)$ equivalence inspires us to infer that the $f(R)$ theory is a serious alternative to GR in understanding gravitation in the universe. We hope that any gravitational phenomenon which calls for MOND in the outer Solar system can potentially be addressed by $f(R)$ gravity theory.

ACKNOWLEDGEMENT

This research has made use of data provided by the International Astronomical Union’s Minor Planet Center.

DATA AVAILABILITY

The orbital data for TNOs, Centaurs and SDOs can be accessed from <https://www.minorplanetcenter.net/data>. The rest of the data underlying this article will be shared on reasonable request to the corresponding author.

REFERENCES

Abercrombie D., et al., 2020, *Phys. Dark Univ.*, 27, 100371

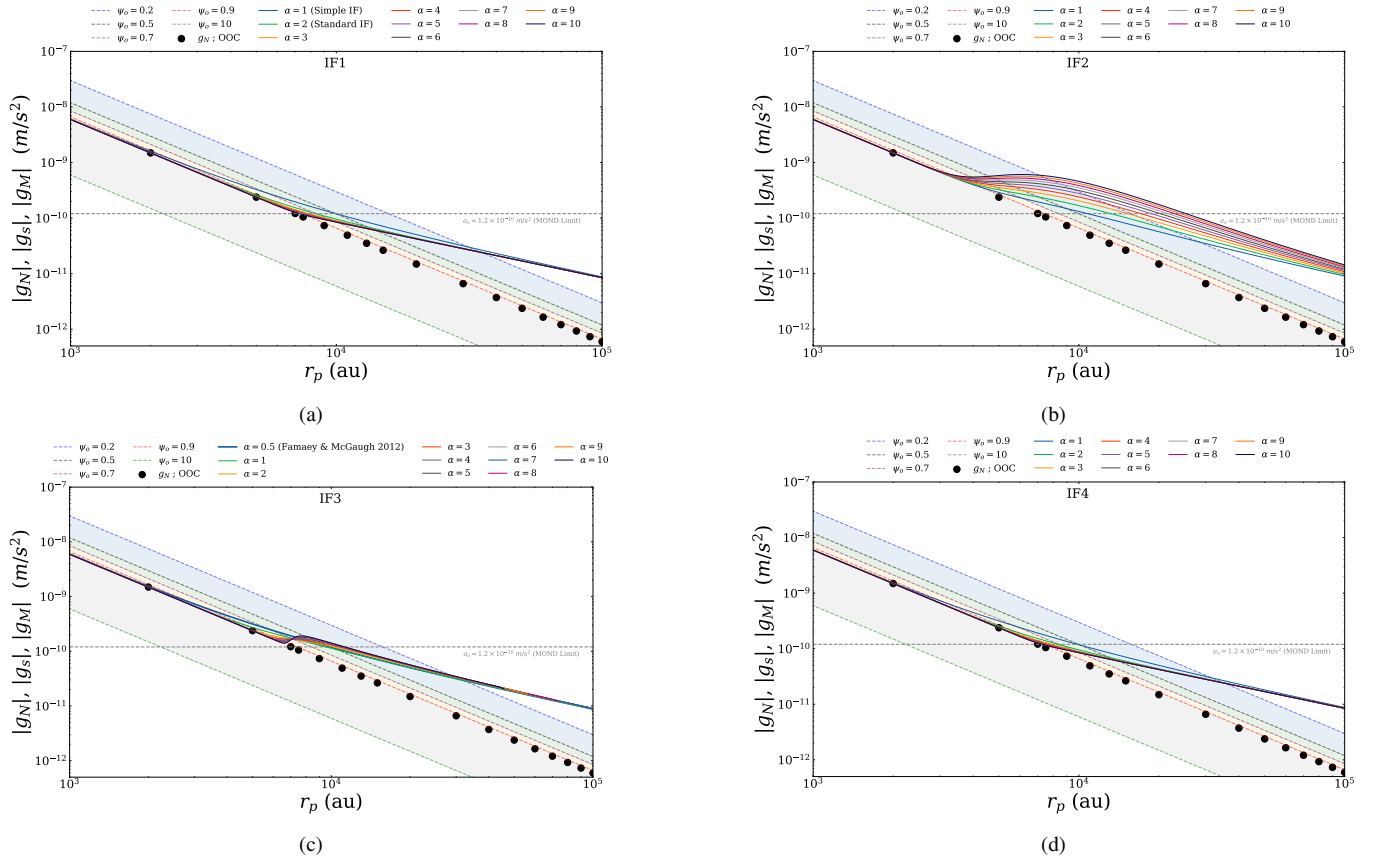


Figure 4. Variation of acceleration due to gravity with respect to perihelion distance in Newtonian, scalaron gravity theory ($\psi_0 < 1$ & $\psi_0 > 1$) and MOND with different family of IFs (A scale of 1000 au - 100000 au has been considered in the above figures as the g_M values deviate from g_N values after around 2000 au for all the MOND IF families).

- Amendola L., 1999, *Phys. Rev. D*, 60, 043501
- Amendola L., Tsujikawa S., 2010, *Dark energy: theory and observations*. Cambridge University Press
- Bartolo N., Pietroni M., 2000, in *Cosmo-99*. World Scientific, pp 91–97
- Batygin K., Adams F. C., Brown M. E., Becker J. C., 2019, *Phys. Rep.*, 805, 1
- Bel J., Brax P., Marinoni C., Valageas P., 2015, *Phys. Rev. D*, 91, 103503
- Bertotti B., Iess L., Tortora P., 2003, *Nature*, 425, 374
- Blumenthal G. R., Faber S. M., Primack J. R., Rees M. J., 1984, *Nature*, 311, 517
- Brans C., Dicke R. H., 1961, *Phys. Rev.*, 124, 925
- Brown K., Mathur H., 2023, *Astron. J.*, 166, 168
- Brown M. E., Trujillo C., Rabinowitz D., 2004, *Astrophys. J.*, 617, 645
- Capozziello S., 2002, *Int. J. Mod. Phys. D*, 11, 483
- Capozziello S., Cardone V. F., Troisi A., 2007, *MNRAS*, 375, 1423
- Carroll S. M., 2001, *Liv. Rev. Relativ.*, 4, 1
- Carroll S. M., Duvvuri V., Trodden M., Turner M. S., 2004, *Phys. Rev. D*, 70, 043528
- Chae K.-H., Bernardi M., Sánchez H. D., Sheth R. K., 2020, *Astrophys. J. Lett.*, 903, L31
- Chan M. H., Lee C. M., 2020, *Phys. Rev. D*, 102, 063017
- Chan M. H., Lee C. M., 2022a, *Phys. Rev. D*, 105, 123006
- Chan M. H., Lee C. M., 2022b, *MNRAS*, 518, 6238
- Chan M. H., Lee C. M., 2022c, *Phys. Lett. B*, 825, 136887
- Copeland E. J., Sami M., Tsujikawa S., 2006, *Int. J. Mod. Phys. D*, 15, 1753
- De Martino I., della Monica R., De Laurentis M., 2021, *Phys. Rev. D*, 104, L101502
- Dutton A. A., Macciò A. V., Obreja A., Buck T., 2019, *MNRAS*, 485, 1886
- EHT Collaboration et al., 2022, *Astrophys. J. Lett.*, 930, L17
- Famaey B., Binney J., 2005, *MNRAS*, 363, 603
- Famaey B., McGaugh S. S., 2012, *Liv. Rev. Relativ.*, 15, 1
- Fienga A., Laskar J., Kuchynka P., Manche H., Desvignes G., Gastineau M., Cognard I., Theureau G., 2011, *Celest. Mech. Dyn. Astron.*, 111, 363
- GRAVITY Collaboration et al., 2018, *Astron. Astrophys.*, 615, L15
- GRAVITY Collaboration et al., 2020, *Astron. Astrophys.*, 636, L5
- Gu J. A., 2011, *Int. J. Mod. Phys. D*, 20, 1357
- Hees A., Famaey B., Angus G. W., Gentile G., 2015, *MNRAS*, 455, 449
- Hees A., et al., 2017, *Phys. Rev. Lett.*, 118, 211101
- Hough R., Abebe A., Ferreira S., 2020, *Eur. Phys. J. C*, 80, 787
- Kalita S., 2018, *Astrophys. J.*, 855, 70
- Kalita S., 2020, *Astrophys. J.*, 893, 31
- Kalita S., 2021, *Astrophys. J.*, 909, 189
- Kalita S., Bhattacharjee P., 2023, *Eur. Phys. J. C*, 83, 120
- Khoury J., Weltman A., 2004, *Phys. Rev. D*, 69, 044026
- LISA Pathfinder Collaboration et al., 2019, *Phys. Rev. D*, 100, 062003
- Lalremruati P. C., Kalita S., 2021, *MNRAS*, 502, 3761
- Lalremruati P. C., Kalita S., 2022, *Astrophys. J.*, 925, 126
- Lelli F., McGaugh S. S., Schombert J. M., Pawlowski M. S., 2017, *Astrophys. J.*, 836, 152
- Li P., Lelli, Federico McGaugh, Stacy Schombert, James 2018, *Astron. Astrophys.*, 615, A3
- March R., Páramos J., Bertolami O., Dell’Agnello S., 2017, *Phys. Rev. D*, 95, 024017
- McGaugh S. S., 2008, *Astrophys. J.*, 683, 137
- McGaugh S., 2020, *Galaxies*, 8
- McGaugh S. S., Lelli F., Schombert J. M., 2016, *Phys. Rev. Lett.*, 117, 201101
- Milgrom M., 1983, *Astrophys. J.*, 270, 365
- Milgrom M., 2009, *MNRAS*, 399, 474
- Misner C. W., Thorne K. S., Wheeler J. A., 1973, *Gravitation*. Macmillan
- Nojiri S., Odintsov S. D., 2003, *Phys. Lett. B*, 562, 147

Table A1. Mock Oort cloud orbits with the mass of scalarons predicted in their respective orbits.

<i>Inner Oort Cloud (IOC) Orbits</i> (2000 – 15000) au			<i>Outer Oort Cloud (OOC) Orbits</i> (15000 – 100000) au		
ID	r_p (au)	M_ψ (eV)	ID	r_p (au)	M_ψ (eV)
<i>IOC1</i>	2000	4.28×10^{-20}	<i>OOC1</i>	20000	4.27×10^{-21}
<i>IOC2</i>	5000	1.71×10^{-20}	<i>OOC2</i>	30000	2.85×10^{-21}
<i>IOC3</i>	7000	1.22×10^{-20}	<i>OOC3</i>	40000	2.14×10^{-21}
<i>IOC4</i>	7500	1.14×10^{-20}	<i>OOC4</i>	50000	1.71×10^{-21}
<i>IOC5</i>	9000	9.50×10^{-21}	<i>OOC5</i>	60000	1.43×10^{-21}
<i>IOC6</i>	11000	7.77×10^{-21}	<i>OOC6</i>	70000	1.22×10^{-21}
<i>IOC7</i>	13000	6.57×10^{-21}	<i>OOC7</i>	80000	1.06×10^{-21}
<i>IOC8</i>	15000	5.70×10^{-21}	<i>OOC8</i>	90000	9.55×10^{-22}
			<i>OOC9</i>	100000	8.55×10^{-22}

- Nyambuya G. G., 2010, *MNRAS*, 403, 1381
 Odintsov S. D., Oikonomou V., Sharov G. S., 2023, *Phys. Lett. B*, 843, 137988
 PICO Collaboration et al., 2016, *Phys. Rev. D*, 93, 061101
 Park R. S., Folkner W. M., Konopliv A. S., Williams J. G., Smith D. E., Zuber M. T., 2017, *Astron. J.*, 153, 121
 Paul D., Kalita S., Talukdar A., 2023, *Int. J. Mod. Phys. D*, 32, 2350021
 Paul D., Bhattacharjee P., Kalita S., 2024, *Astrophys. J.*, 964, 127
 Peebles P. J. E., 1982, *Astrophys. J. Lett.*, 263, L1
 Peebles P. J. E., 2015, *Proc. Natl. Acad. Sci.*, 112, 12246
 Peebles P. J. E., Ratra B., 2003, *Rev. Mod. Phys.*, 75, 559
 Perlmutter S., et al., 1999, *Astrophys. J.*, 517, 565
 Riess A. G., et al., 1998, *Astron. J.*, 116, 1009
 Rubin V. C., Ford W. Kent J., 1970, *Astrophys. J.*, 159, 379
 Rubin V. C., Ford W. K. J., Thonnard N., 1978, *Astrophys. J. Lett.*, 225, L107
 Sahni V., Starobinsky A., 2000, *Int. J. Mod. Phys. D*, 09, 373
 Sanders R. H., Noordermeer E., 2007, *MNRAS*, 379, 702
 Stabile A., Capozziello S., 2013, *Phys. Rev. D*, 87, 064002
 Starobinsky A., 1980, *Phys. Lett. B*, 91, 99
 Starobinsky A. A., 2007, *JETP Lett.*, 86, 157
 The Fermi-LAT Collaboration et al., 2015, *Phys. Rev. Lett.*, 115, 231301
 Wang L., Chen D.-M., 2021, *Res. Astron. Astrophys.*, 21, 271
 Weinberg S., 1989, *Rev. Mod. Phys.*, 61, 1
 Will C. M., 2014, *Liv. Rev. Relativ.*, 17, 1
 Wilson C., Bean R., 2021, *Phys. Rev. D*, 104, 023512
 XENON Collaboration et al., 2018, *Phys. Rev. Lett.*, 121, 111302
 Xu T., Cao S., Qi J., Biesiada M., Zheng X., Zhu Z.-H., 2018, *J. Cosmol. Astropart. Phys.*, 2018, 042
 Zhao H. S., Famaey B., 2006, *Astrophys. J.*, 638, L9

APPENDIX A: MOCK OORT CLOUD ORBITS

Some mock Oort cloud orbits have been considered and the mass of scalarons in their respective orbits have been estimated using equation 7. The mock data have been presented in Table A1.

This paper has been typeset from a \LaTeX file prepared by the author.